Chapter 2 in "*Multiphase Bioreactor Design*", J.M.S. Cabral, M. Mota, J. Tramper (Eds.),
Taylor & Francis, London, 25-52, 2001.

Image Analysis and Multiphase Bioreactors

Eugénio Campos Ferreira[1], Manuel Mota[1], and Marie-Nöelle Pons[2]
[1]Centro de Engenharia Biológica – IBQF, Universidade do Minho, 4710-057 Braga, Portugal
[2]Laboratoire des Sciences du Génie Chimique, CNRS-ENSIC-INPL, rue Grandville BP 451, F-54001 Nancy cedex, France

ABSTRACT

The applications of visualisation and image analysis to bioreactors can be found in two main areas: the characterisation of biomass (fungi, bacteria, yeasts, animal and plant cells, etc), in terms of size, morphology and physiology, that is the far most developed, and the characterisation of the multiphase behaviour of the reactors (flow patterns, velocity fields, bubble size and shape distribution, foaming), that may require sophisticated visualisation techniques.

Keywords Image Analysis, Morphology.

INTRODUCTION

Vision, on the opposite of other senses, may be the only sense that provides holistic sensorial information. In a glance, we perceive a whole set of characteristics of an object: its distance, its motion, its colour, its shape, its size, its texture, its brightness and its transparency. Therefore, it is not surprising that the area of the brain cortex dedicated to vision is bigger than the areas allocated to the other senses.

Man has identified ten regions of the occipital lobe of the brain related to vision and, today, the functions of some are still unknown (Logothetis 1999). On that matter, Kandel, Schwartz and Jessel (1995) state: «We have learned that contrary to the intuitive analysis of our personal experience, perceptions are not precise and direct copies of the world around us. Sensation is an abstraction, not a replication of the real world. The brain does not simply record the external world like a three dimensional photograph. Rather, the brain constructs an internal representation of external physical events after first analysing them into component parts. In scanning the visual field the brain simultaneously but separately analyses the form of objects, their movement and their colour, all before putting together an image according to the brains' own rules. How this reconstruction occurs – the binding problem – is one of the most previous questions in cognitive neural science.»

Nevertheless, vision's holistic properties have obvious advantages in the information storage and interpretation.

Thus, according to the saying "an image speaks louder than a thousand words", various areas of knowledge have used images to represent complex phenomena in a condensed manner. That is the case, for example, of medical imagiology, or of the process of making tri-dimensional computerized models in fluid dynamics (CFD), nowadays widely used in the design of aerodynamic surfaces or in the study of mixing phenomena in bioreactors.

The development of great capacity automatic systems, provided by the increase of the computer processing capacity, on the one hand, and the acknowledgement of the importance of some parameters not very "quantifiable" in the performance of some industrial processes – agglomeration, roughness, brightness and morphology, among others – has been encouraging the development of another aspect of vision, that is, the capacity of perceiving and comparing complex processes, allowing its control, without having to use complex model equations, which are sometimes impossible to develop.

This side of image acquisition and analysis has been raising interesting problems to the very research of the mechanisms involved in the human vision, namely in the area of robotic vision: matters as segmentation, perception, recognition and memory concern automatic vision, as well as human vision. In deed, and according to Hans Moravec (1999), the present velocity of microprocessors is still very slow. Moravec defends that «…from long experience working on robot vision systems, I know that similar edge (to retina) or motion detection, if performed by efficient software, requires the execution of at least a hundred computer instructions. Thus, to accomplish the retina's ten million detections per second would require at least a thousand MIPS (million instructions per second).» And he proceeds further on: «Perhaps by 2010 the process will have produced the first broadly competent "universal robots", as big as people but with lizardlike 5000 MIPS minds that can be programmed for almost any simple chore.»

The methodology of image acquisition and analysis will, therefore, invade all areas where quick and condensed processing of information shows to be critical. This is one of the characteristics of biochemical engineering, where the control of biological processes occurring in a bioreactor, involves a very large number of variables interacting simultaneously.

We are now going to discuss this subject and its evolutions.

IMAGE PROCESSING

If an image can be immediately understood by a human being, the quantification of the information it contains is far more difficult especially on a large set of images. Automated image processing plays that role, but obviously the image treatment will depend upon the type and quality of the image and the goal of the final user of the quantification. Nevertheless, it is possible to define a series of basic steps which can be found in any image analysis procedure (Figure 1).

The image processing starts with the visualisation step. Different devices can be used: for biomass characterisation optical microscopes are the most common tools but a large range of imaging methods can be used for the hydrodynamic behaviour characterisation. Generally an electronic eye (camera) is substituted to the human eye. The video signal is further processed into a digital one, the image, i.e. a set of picture elements (= pixels) arranged according to lines and columns. It is important to note that an image is a projection onto a plane of a reality, which is 3-dimensional. In most applications, especially for biomass characterisation, the quantification will be made on projections. It will be seen later that it is possible to obtain 3D information, especially for hydrodynamic applications, to the expense of more sophisticated imaging systems. Generally, for routine applications, the imaging process is less expensive for biomass characterisation.

The digital image which has been captured is a grey-level image: the value assigned to each pixel is directly connected to the amount of transmitted or reflected electromagnetic energy and is generally coded on 8 bits, giving 256 grey levels or sometimes, for applications related to fluorescence or luminescence, on 12 bits (4096 grey levels). A colour image is a combination of three images, each one corresponding to one of the primary colours: Red, Green and Blue (RGB colour system).

Some images will be directly used as grey level images: it is the case for densitometry studies (tomography and radiography) or characterisation of visual textures (foams). Generally however the amount of information contained in the grey level images is so large that a simplification is needed: a segmentation between the objects of interest and the background is performed leading to binary images with just two grey levels: 1 for the objects, 0 for the background. Although the

highest care should be taken in the visualisation step for getting good quality images, some enhancement of the grey level images may be necessary at this stage. However, this enhancement should be minimised, since most of those treatments will introduce some bias in the final results.
Many procedures exist for the segmentation: it is recommended to use an automated or at least semi-automated algorithm, to reduce the interference with the operator. It is possible to segment colour images by triple threshold on the three primary colours, although the transformation into the Hue-Saturation-Intensity (HSI) colour system, closer to the human vision, is recommended: on epifluorescence images the segmentation in the Intensity plane gives directly the background (black i.e. with a low brightness level) and the objects. The colour characterisation will be conducted by combining the obtained binary image with the information contained in the Hue plane. The binary image may require some cleaning: removal of debris, especially with complex culture media, of objects in contact with the image frame, hole filling, etc. Finally the image is prepared to proceed to the next step, quantification that will greatly depends upon the application.

BIOMASS CHARACTERISATION

Filamentous fungi and filamentous bacteria

Fungi and filamentous bacteria have been used to produce a range of important metabolites such as antibiotics, organic acids, proteins, enzymes, food and other chemicals. In submerged cultures they may grow either as disperse form (dispersed hyphae and clumps in a free mycelium) or as pellets that are resulting from the entanglement and aggregation of filamentous mycelium. The morphology of filamentous microorganisms was reviewed by Nielsen (1996) and Thomas (1992).
The main objective is, in any application, the classification according to the morphological type (i.e. dispersed hyphae, clumps and pellets) with a more precise description of each individual within its class. Dispersed hyphae are characterised generally by the total hyphal length, the number of tips (apices) and branching points, the main hyphal length, and the mean branch length. The hyphal growth unit (HGU) is given by the ratio of the total hyphal length to the number of tips. Clumps are often described by the ratio of their projected surface to the surface of the convex bounding polygon. Pellets are characterised by their total projected areas and the projected area of the hairy crown or the core. Durant and co-workers (Durant et al 1994; Durant, Crawley and Formisyn 1994) improved the discrimination between filamentous regions and compacted cores, by staining mycelial aggregates of *Basidiomycetes* with crystal violet.
Once again it has to be reminded that an image is a 2D projection of a 3D reality and that only a single projected surface can be obtained directly. Assumptions on the 3D shape have to be made to obtain volume-based information: this is typically the problem for pellets. In each morphological class, average values have to be calculated on a meaningful number of individuals. Tables 1 and 2 give examples of applications to fungi and filamentous bacteria.
Staining techniques associated to image analysis (IA) are becoming ubiquitous for the examination of active regions of hyphae and physiological characterisation. The first attempt to quantify the proportion of growing apices in *Penicillium chrysogenum* was made by Paul, Kent and Thomas (1994) by using neutral red staining. A quantitative method was later developed (Vanhoutte et al 1995) for a more detailed characterisation of the physiology of *P. chrysogenum*. It was based on a differential staining procedure showing six physiological states: growing

material, three differentiated states with an increasing granulation, a highly vacuolized state, and dead segments having lost their cytoplasm. More recently, Cox and Thomas (1999) used a fluorescent stain (Mag fura) to evaluate the active hyphal regions of two industrial strains of filamentous fungi (*P. chrysogenum* and *Aspergillus oryzae*).
Streptomyces hyphae are thinner than the fungal ones, and the magnification normally used in optical microscopy do not allow the cytoplasm visualisation. Nevertheless, staining can bring valuable information for those bacteria strains. To understand relations between cellular differentiation of *Streptomyces ambofaciens* in submerged culture (Figure 2), and spiramycin production, Drouin et al (1997) used IA. Three parameters were measured: occurrence of empty zones in mycelium, number of septations, mycelium thickness. Previously, the same group used IA for localising the respiration sites based on the distribution of formazan crystals along the hyphae. Recently, Sebastine et al (1999) developed an IA method to identify the different physiological states of *Streptomyces clavuligerus* using a fluorescent bacterial viability stain, a mixture of SYTO9 and propidium iodide.

Non-filamentous bacteria

Problem of non-filamentous bacteria imaging lays in the small size of the microorganisms. In spite of this, Dubuisson, Jain and Jain (1994) employed IA and pattern recognition techniques to count and identify cultures of methanogens (*Methanospirillum hungatei* and *Methanosarcina mazei*). In anaerobic wastewater digesters, flocs and granules are bacterial aggregates whose size (Dudley et al 1993) and roughness (Bellouti et al 1997) can be monitored by IA and related to the efficiency of the reactors. Settleability of activated sludge can be characterised by the fractal dimension of the flocs (Grijspeerdt and Verstraete 1997).
The main routine applications are dealing with viability assessment using such vital stains as Orange Acridine, and epifluorescence microscopy (Singh, Pyle and McFeters 1989).
The emergence of new fluorescent phylogenetic probes combined with microscopic techniques allows the assessment of the identities and activities of bacterial cells within complex microbial communities. Automated Confocal Laser Scanning Microscopy (CLSM) combined with image processing techniques allowed the assessment of 3D biofilm structures (see chapter "Fixed Film Bioreactors" in this book) under in situ conditions (Kuehn et al 1998) and off line sampling from a rotating annular bioreactor (Lawrence, Nie and Swerhone 1998).
When Fluorescence In Situ Hybridisation (FISH) was combined with CLSM this approach allowed visualising spatial organisations of microbes in methanogens granules (Sekiguchi et al 1999) of upflow anaerobic sludge blanket reactors. Properties of a synthetic biofilm (*Escherichia coli*) were examined by using CLSM in combination with fluorescent probes (Swope and Flicklinger 1996). Combination of FISH and microautoradiography enabled the assessment of the structure and function of bacterial communities (Lee et al 1999), specially in activated sludge processes (Nielsen et al 1999; Kawaharasaki et al 1998).

Yeasts

The yeast *Saccharomyces cerevisiae* is widely used in biopharmaceutical and food processes. Some authors have developed IA techniques for sizing and counting of *S. cerevisiae* (Vicente, Meinders and Teixeira 1996, Yamashita et al 1993, Costello and Monk 1985). Besides cell counting, morphological properties can be used to estimate physiological condition of yeast cultures especially related to cell budding and division (Hirano 1990) and vacuolisation (Zalewski and Buchholz 1996). A semiautomatic method was proposed by Pons et al (1993) to

characterise the morphology of yeast cells (see Figure 3). Yeast size distributions and population kinetics (single and budding cells, cell clusters) were determined during alcoholic fermentations.
Walsh et al (1996) determined geometric properties of immobilised *S. cerevisiae* microcolonies in alginate and carrageenan gel particles. IA provided measurements of the cross-sectional area and aspect ratio of each microcolony and the distance of the centroid of the microcolony from the centre of the cross-section.
O'Shea and Walsh (1996) applied IA to separate cells of the yeast *Kluyveromyces marxians* into six defined categories (from ovoid cells to branched mycelial cells). These dimorphic yeast cells were used in an alcoholic fermentation of cheese whey permeate. This research was recently updated (Mccarthy et al 1998) with the cell morphology characterisation and its effect on dead-end filtration.
IA techniques were utilised (Perrier-Cornet, Maréchal and Gervais 1995) in a high-pressure optical micro-reactor to calculate cell volumes on individual cells of *Saccharomycopsis fibuligera*. Cells were assumed to be spherical and the projected area was accessed by IA on pictures taken on an inverted light microscope.
Machine vision microscopy systems have been proposed for yeast cell culture visualisation, usually employing an automatic sampling device for delivering the sample to the viewing stage of the microscope (Ren, Reid and Litchfield 1994, Zalewski and Buchholz 1996). In-situ microscopes were developed for on-line characterisation of *S. cerevisiae* (Suhr et al 1995; Bittner, Wehnert and Scheper 1998). Cell concentration and cell size were estimated using a microscope mounted in a port of a bioreactor. Guterman and Shabtai (1996) proposed a machine vision system combined with neural networks and fuzzy logic techniques to recognise changes of population distribution of the yeast-like fungus *Aureobasidium pullulans*.

Animal cells

A real-time imaging system was presented by Konstantinov et al (1994) for cell counting and sizing of animal-cell culture in a bioreactor. An *in situ* microscopic image analysis system was developed by Maruhashi, Murakami and Baba (1994) to automate measurements of cell concentration and viability in a suspended animal cell culture (mouse-mouse hybridoma STK1).
At Novo Nordisk pilot plant an IA software was developed (Bonarius, Nielsen and Kongerslev 1997) for monitoring the cell density in Chinese hamster ovary (CHO) cell cultures. Neural networks were used to distinguish stained nuclei from cell debris and other objects in the image.
Ruaan, Tsai and Tsao (1993) reported the application of video IA for the on-line monitoring of CHO growth using an inverted microscope and a flow system. Local cell density, cell motility, and cell surface area were continuously estimated. Tucker et al (1994) proposed an IA method for characterising the viability and morphology of hybridoma cells from suspension cultures. The total and viable cell counts and the percentage of dead cells present were found using the exclusion dye Trypan Blue.
IA was applied to the monitoring of cultures of human kidney tumour cells: procedures were developed to investigate microcarrier colonisation, cluster formation and cell size using scanning electron microscopy (Pons et al 1992) and optical microscopy (Pichon, Vivier and Pons, 1992) as illustrated in Figure 4.
The total surface area occupied by a variety of mammalian cell lines, and the number of cells attached to fibronectin and a fusion protein (CBD/RGD) were evaluated using IA techniques (Wierzba et al 1995).
Chalmers and Bavarian (1991) presented a microscopic, high-speed video system to study the interactions of two suspended insect cells strains with bubble film and bubbles rupturing. A

fluorescence microscopy technique was used by Cowger et al (1999) to characterise the distribution of necrotic and apoptotic insect cells in a rotating-wall vessel. The distribution was based on staining pattern and morphology.

Plant cells (and suspended somatic embryos)

Bioreactor technology provides the potential for producing large numbers of plants more cheaply and efficiently (Cazzulino, Pedersen and Chin 1991) than tissue culture on agar solidified medium or through the use of shake flask cultures. Diverse varying plant morphologies may be observed in cell cultures as illustrated in Figure 5: single cells, cell aggregates, and organised plant structures from different stages of embryogenesis, ranging from globular to torpedo. The heterogeneous mixture of cells needs to be quantified for evaluation of the conditions promoting good development of culture. IA technology provides one practical solution to the problem of characterising the morphology of somatic embryos in culture.
Recently, applications of image analysis in large scale plant micropropagation (during somatic embryogenesis) were reported: machine vision systems were used for the on-line growth monitoring of callus suspension cultures of *Ipomea batatas* in an airlift bioreactor (Harrell, Bieniek and Cantliffe 1992) and of pigment-producing *Ajuga* cells (Smith et al 1995). Uozumi et al (1993) distinguished several morphological classes in liquid suspension cultures of celery through a pattern recognition technique based on neural networks; a similar approach was used by Chi et al (1996) in liquid suspension cultures of carrot; Cazzulino, Pedersen and Chin (1991) developed IA procedures that enables the routine characterisation of carrot somatic embryos in a liquid culture. Shape recognition algorithms (multilevel simple statistical comparisons and classificatory discriminant analysis) were employed for microscopic observations of the different embryo stages. Honda et al (1999) used the trichromatic colours (RGB) to distinguish between two kinds of sugarcane calli on solid media; Barciela and Vieitez (1993) determined morphological parameters on cultured cotyledon explants of *Camellia japonica*.
Kieran, Malone and Macloughlin (1993) used IA to evaluate cell length, chain length and number of cells per chain in suspended cultures of *Morinda citrifolia* in batch and semi-continuous stirred tank reactor. Those properties were identified as useful indicators of the influence of stirrer speeds on the morphology of the cultures in the early exponential growth phase. These authors (Kieran et al 1995) also evaluate the effect of fluid shear susceptibility on the morphology.

Protozoa and other higher life forms

Protozoa, rotifers, nematodes (see chapter on "Nematode Bioreactors"), etc are microorganisms involved in the good operation of wastewater treatment plants by activated sludge (Jenkins, Richard and Daigger 1993). This can be assessed by a Sludge Biotic Index (Madoni 1994), which requires the counting, and recognition of the various members of the microfauna. Automation of this tedious task would be of great help for plant operators: some success in this direction has been obtained recently by Amaral et al (1999). Figure 6 illustrates some examples of digitised images of protozoa species in wastewater activated sludge.
An IA system was developed by Kaneshiro et al (1993) for the viability assessment of protozoa using a fluorescent staining technique.

BIOREACTOR IMAGING

Bioreactors are essentially multiphase systems in which the mass (and in some processes the heat) transfer is a key issue. The characterisation of mixing has received therefore a lot of attention. Traditionally residence time distributions obtained by inert tracer injection have been used for liquid, gas, and more seldom solid phases (Tatterson, 1991; Lumley and Horkeby, 1989).

Imaging methods have been developed, which provide two types of information:

- The global characterisation of the mixing, where the 2D or 3D distribution of at least one of the components of the multiphase system is given: the changes of a physical property with respect to the component concentration are monitored.
- The characterisation of flow patterns and velocity fields by tracking the motion of individual particles

Here the term of imaging has to be understood in its widest sense, meaning that light is not the only excitation beam.

Tomography and radiography enable non-invasive characterisation of multiphase flows. An excellent review is provided by Chaouki, Larachi and Dudukovic (1997). The selection of the excitation signal depends on the contrast of the chosen physical property between the different phases:

- Nuclear-based with ionising radiations, essentially γ and X rays. Neutron imaging is mostly used for reactive flows in consolidated porous media, therefore outside the scope of bioreactors.
- Nuclear-based with non-ionising radiations such as Nuclear Magnetic Resonance (NMR), which has been used for many years in medical applications. Proton NMR is particularly suited because water is abundant in biological systems, but other nuclei might be of interest, such as ^{31}P and ^{23}Na, to monitor biological activities (DiBiasio *et al* 1993; Sardonini and DiBiasio, 1993).
- Non nuclear-based: electrical capacitance, optical radiation, ultrasound, and microwave.

The difference between tomography and radiography lays in the detection system: the attenuation of the beam is registered by discrete detectors in the case of tomography when a sheet of film or a camera is used for radiography (Figure 7a). For tomography different arrangements have been proposed, with single or multiple, displaceable, sets of sources and detectors. The visualisation takes usually place in a plane.

In both methods the beam transmitted through the medium is attenuated depending upon the distribution of the sensitive physical property, *f*, along the path traversed by the beam. The collected signal, *P*, is a 2D projection of a 3D reality:

$$P(l,\theta) = \int_L f(x,y)ds$$

Different reconstruction algorithms (Kumar and Dudukovic, 1997; Godfroy *et al*, 1997; Reinecke *et al*, 1998) have been proposed to back-calculate *f* from *P* (Figure 7b).

The quality of the imaging is function of the spatial, temporal and density resolution. Spatial resolution is the minimum distance that two objects can be separated. With sets of detectors it depends upon their number, spacing and size: X-rays require smaller detectors than γ-rays. But the latter are more penetrating and can be used with larger test sections. With a camera, the spatial resolution depends upon the adequateness between the reactor size and the number of lines and pixels/line of the resulting image. With NMR the size of the bioreactor to be imaged is limited by the size of the magnet's bore. Temporal resolution is the basic limitation in X-rays and γ-rays tomography, due to the necessity to rotate the sources and/or the detectors to obtain

the photon count rates for all the projections. Dynamic information can be obtained only when the flow characteristics change sufficiently slowly. This drawback does not exist with electrical capacitance or resistance tomography that is much faster (and safer!): however its spatial resolution is poorer although improvements have been made recently (Holden *et al* 1998). Density resolution refers to the smallest difference in the measured physical property that the system is able to distinguish. Optical methods require transparent media. Distortion effects are introduced by light diffraction phenomena: thin two-dimensional vessels are designed and cylindrical reactors are embedded in rectangular optical boxes. Hari-Prajitno *et al* (1998) have used a starch/iodine solution decolourised by injection of sodium thiosulfate to determine the mixing times in multi-impeller systems. Galindo and Nienow (1992, 1993) introduced methylene blue near the impeller to investigate the mixing characteristics of various devices in simulated xanthan gum broths. A similar technique is employed by Bujalski *et al* (1999) to examine the suspension and liquid homogenisation in stirred tanks containing solids. In bioprocesses these solids could be microcarriers in cell cultures or sludge for wastewater treatment (Schaflinger, Acrivos and Zhang, 1990). Figure 8a presents schematically a set-up to study the resuspension of sludge in sequencing batch bioreactors with surface aeration for wastewater treatment. The sludge is simulated by carboxymethylcellulose (CMC) solutions dyed with methylene blue. Clear water is poured above the CMC layer in the tank with care to avoid any mixing of the two layers. At time zero the impeller, here a Rushton turbine, is set into motion. After a lag phase, which is a function of the CMC concentration, i.e. the compactness of the sludge that may result from an extended settling period, the viscous layer is gradually mixed with the water layer. The mixing is monitored with a camera connected to a videotape recorder. The images are later digitised (Figure 9). The variation of the grey level within areas of interest enables to follow the progress of the mixing (Figure 8b).

Houcine *et al* (1996) characterised the mixing in a plane defined as the cross section of the flow by a thin laser sheet, which excites the fluorescence of a non-reacting tracer (Figure 10a). The instantaneous field of dye concentration is obtained automatically from the digitised video images. Experiments in a continuous stirred tank have been run with two inlet sources: a contacting parameter which emphasises the average state of mixing and the field of temporal variance, which characterises the segregation of the investigated zone, are computed. This can be a useful technique to study the dispersion of highly concentrated nutriments or pH reagent streams in bioreactors. Other methods of data analysis such as 3D-wavelets have been proposed to help the comparison between systems (Li and Wei 1999).

Velocimetry techniques use electromagnetically active particles, sensitive to nuclear radiations or visible or fluorescent light and which are able to mimic the motion of a flow particle. In positron emission trajectography (PET), particles are produced by direct irradiation of a particle in a cyclotron, by adsorption of a radioisotope on the tracer surface or by manufacturing a particle out of a radioactive material, but the detection systems able to reconstruct the trajectory of the particle are complex and expensive. A simpler radioactive particle tracking method makes use of β^- emitters produced by neutron capture. Different triangulation procedures have been developed to determine the 3D co-ordinates of the particles from the counts given by the detectors (Figure 10b).

In spite of distortion effects to be corrected, optical tracking of particles is more affordable. Different variants exist:

- Particle Imaging Velocimetry (PIV): the velocity of particles are calculated by correlating the displacements on a double exposure image

- Particle Streak Velocimetry (PSV): on a long-exposure image sections of the particles trajectory appear as streaks. However the particles should not leave the plane of focus and the particle density is much lower than with PIV.
- Particle Tracking Velocimetry (PTV): the motion of the particle is recorded by a video camera

A 3D-PTV system has been developed by Wittmer *et al* (1995) and Pitiot, Falk and Vivier (1998) to study the mixing characteristics in mixed reactors with Newtonian and non-Newtonian fluids for different agitation systems (Figure 11). Two (or three) monochrome video cameras monitor the displacement of the particle, each camera being connected to one colour channel of an electronic encoder that delivers colour images (PAL format). This allows for a perfect synchronisation of the video signals. The colour images are digitised on a PC equipped with a special board for real-time image capture at the rate of 25 frames per second. One of the key problems is the quality of the particle, the buoyancy of which should be adapted with respect to the density of the fluid. Pitiot, Falk and Vivier (1998) manufacture their gelatine-based particle by micro-encapsulation: the particle self-adapts its buoyancy by diffusion of the bulk liquid phase through the particle wall. Figure 12 compares the effect of some rheological properties on the trajectory of the particle in a stirred tank equipped with a Mixel mobile. A single camera is used by Venkat *et al* (1993) to track the motion of microcarriers in spinner vessels, but a suitable arrangement of mirrors enable a stereo-vision of the particles on a single image on a high-speed film (400 frames per sec). Another key issue is the spatial resolution: Pitiot's particles have a diameter of about 2 mm for a reactor diameter of 300 mm. Micro-carriers are smaller (about 200 μm) and the field of view is restricted to a portion of the spinner vessel.

Aerobic systems represent the largest group of commercial reactors. Bubbles transfer oxygen to microorganisms and remove carbon dioxide. The transfer is improved by high specific surfaces, corresponding to small bubble sizes. However liquid rheological properties and vessel geometry induce generally bubble size distributions. Large bubbles produced by coalescence are found near the surface, where gas disengages. Bubbles near walls are also larger than in the vicinity of impellers (Calderbank, 1958, Takahashi and Nienow, 1988). There is a need to characterise better the phenomena taking place around the bubbles to improve the scale-up of bioreactors, either mechanically agitated or flow contactors (air-lift, bubble columns).

When the bubble density is high, only the bubbles in the vicinity of the wall are considered. Some authors use two-dimensional column (de Swart, van Vliet and Khrisna 1996, Atenas, Clark and Lazarova 1998). To avoid blurring, a small shutter speed and flashlights are employed. When bubbles are almost spherical, their size distribution is obtained easily (Bouaifi and Roustan 1998). But bubbles can deflect largely from spheres (de Swart, van Vliet and Khrisna 1996) as seen in Figure 13. For rising bubbles, especially in viscous fluids like polysaccharide broths, the assumption of a vertical axis of symmetry enables to calculate their volume (Mouline 1996; Margaritis, te Bokel and Karamanev 1999). A Fourier analysis of the silhouette contour of bubbles was used by Atenas, Clark and Lazarova (1998) to investigate the shape of bubbles in a rectangular airlift bioreactor. Fourier analysis is usually rather cumbersome and more classical shape parameters, as those used to assess solid particle morphology (elongation, circularity, concavity index), may be useful in a first approach (Pons *et al*, 1999).

Bubbles shape and velocity can change with time. This has been studied by Benkrid (1999) in a 2D column using a high-speed camera (500 to 1000 i/s) and co-currents of gas and newtonian liquid. Gobal and Jepson (1997) work at a lower rate (30 i/s) but separate the two frames of each image, obtaining finally a rate of 60 f/s, in their study of velocity and void profiles in slug flow. Bubbles can break against various obstacles in the bioreactor, such as probes or immersed heat exchanger tubes (Pandit, Dodd and Davidson 1993). Coalescence of bubbles in non-newtonian

fluids has been investigated by Mouline (1996) and Li *et al* (1997). The generation of bubbles at a sparger orifice (Figure 14) or at the surface of a membrane (Semmens *et al*, 1999) can be studied with the same techniques.

To look in more details at the mass transfer in the vicinity of a bubble, Schmidt and Lübbert (1993) immobilise a nitrogen bubble in a vertical conical tube through which water flows downward. A pH-indicator, phenolphthalein, has been dissolved in the water. Ammonia is injected through the bubble by a thin capillary: ammonia is transferred to the liquid phase via the gas-liquid interface and the pH-indicator turns red. The reaction is monitored via a camera and takes place in the wake of the bubble.

Bursting of bubbles has received a special attention in animal cell cultures, and to a smaller extent in plant cell cultures (Doran, 1999). These cells are susceptible to damage by mechanical agitation and/or gas sparging. Two phenomena are taking place: bubble coalescence and break-up at the free gas-liquid interface; shear stresses arising from high agitation speeds of the bulk liquid with Kolmogorov eddy sizes similar to or smaller than the cell sizes. Protective effect of serum and Pluronic F-68 has been noticed by many researchers (Tan *et al*, 1993). The first visualisation of bursting bubbles has been reported by Rayleigh (1891). Bavarian, Fan and Chalmers (1991) and Chalmers and Bavarian (1991) describe how insect cells get attached to bubbles and are killed by the rapid acceleration of the bubble film after its rupture at the surface and by the high levels of shear stress in the boundary layer flow associated with the bubble jet formation. Furthermore the experimental shape of the jet can be compared to profiles given by simulation models and related to energy dissipation rates (Boulton-Stone and Blake 1993, Garcia-Briones and Chalmers 1993).

Fermentation media are usually prone to foaming, which causes problems of overflow and entrainment of liquid in the gas events. Foam control is usually done by addition of antifoams, which change the surface tension of the liquid and the coalescence behaviour of bubbles in the foam and in the liquid, affecting in that way the gas dispersion and the oxygen mass transfer coefficient. Furthermore antifoam can be poisonous for microorganisms. In an aerobic fermentation, the foam is produced continuously: if the foam height is constant, it means that the rate of bubble bursting at the top surface is equal to the rate of bubble formation at the layer base. Foams can be very different from their structure and bubble size distribution. Foams with bubbles of 2-3 mm in diameter or smaller, with a rather high liquid volume fraction (higher than 0.3) have bubbles that can be considered as spherical or slightly ellipsoidal. Foams with larger bubbles or small bubbles but with a low liquid volume fraction have polyhedral shapes.

The concept of foaminess characterises the foam forming properties of a solution. It is easily calculated from the height of the foam layer produced by a steady rate of gas in a column and monitored by a camera (Lee *et al* 1993). The structure of the foam is more difficult to characterise because the image represents a set of objects in contact. One way to treat the problem is to appreciate quantitatively the visual texture: the challenge is to quantify the regularity, the fineness, the homogeneity, and the orientation of the textural patterns. This approach is extensively used in spatial and aerial imaging but applications can also be found in process engineering. The control of ore flotation can be automated by quantitative analysis of the visual texture of the froth (Moolman, Aldrich *et al* 1994). The analysis is directly conducted on the grey-level images. A very simple approach consists in classifying the images according to some properties of their grey-level histogram (mean, mode, standard deviation). Flow patterns (single phase, bubbly flow, slug flow, churn flow) in a circulation loop have been discriminated based on the simple examination of their histograms (Hsieh, Wang and Pan 1997). But the methods which seem to be the most useful in that field are based on the analysis of the grey level run length (GLRL) matrices and the spatial grey level dependence (SGLD) matrices (Haralick

1979, Conners 1980) where the grey-level neighbourhood of each pixel is taken into consideration.
In the SGLD method a co-occurrence grey-level matrix C (c_{ij}) of dimension N_g x N_g, where N_g is the maximal number of possible grey levels (usually 256) is defined as:

c_{ij} = frequency of occurrence of having a pixel of grey level j at a distance d and angle α of a pixel of grey level i. The C matrix is itself characterised by descriptors based on the c_{ij} such as inertia, entropy or energy. Generally it is useful to combine these techniques with a pattern recognition procedure, such as a principal component analysis of the descriptors (Einax, Zwanziger and Geiss 1997). This enables a rapid comparison of the structures. The pattern recognition procedure consists in a training phase with reference textures and a validation phase. As an example several textures from Brodatz (1966) have been scanned. These textures have some visual similarities with foams. Foam images from a test column have also been obtained under various experimental conditions. All considered images as having a size of 256x256 pixels. The co-occurrence matrices have been computed for d = 5 pixels and for α = 0°, 45°, 90° and 135°. The descriptors have been averaged over the four values of α. A map with the relative positions of the different textures, showing the similarities and dissimilarities can be found in Figure 15. Similarly Sarker *et al* (1998) compare air-water foams prepared with different surfactants (proteins and emulsifiers) in a test column by combination of the GLRL method and a principal component analysis of the texture descriptors calculated on the GLRL matrices.

CONCLUSION

The current applications of image analysis will be enlarged. For example, it does not belong to the field of utopia to consider in the near future the utilisation of sophisticated morphometric techniques able to automatically identify and count the different kinds of microorganisms present in an optical microscopic field, or to determine the state of a sporulant culture.
On the other hand, IA will still be useful to condense information coming from different types of acquisition systems: 3-D NIR/FTIR spectra, confocal imaging, or simple optical "in situ" microscopy combined with adequately chosen chromophores or fluorophores, which will enable in depth dynamic physiological studies of cellular phenomena.
Still, one may easily imagine more progresses in the years to come. Indeed, if, along life's evolution on Earth, several kinds of vision systems - eyespots, ocelli, compound eyes, camera-like eyes, among others - were retained following the implacable sieve of natural selection for millions of years, there will certainly be advantages and drawbacks in each vision system mother nature has finally adopted.
This line of research has not been deeply exploited so far, since the advantages of each vision system are not fully understood yet.
The mammal vision system is organised in such a way that different image properties are processed in different brain areas (Kandel, Schwartz and Jessel 1995). Since the neuronal responses are distributed among different cortex levels, neuroscience is currently investigating how the distinct levels relate themselves and interact to achieve the perceptual construction of an object. This is the well-known binding problem. Nowadays it is universally accepted that image perception in mammals comes from a sophisticated parallel processing of information. It is thus natural that parallel processing will also be a fertile field of research for new developments in image analysis (Leondes 1998).
We may therefore conclude that Image Analysis will develop even further in the near future.

REFERENCES

Amanullah, A., Blair, R., Nienow, A.W. and Thomas, C.R. (1999) Effects of Agitation Intensity on Mycelial Morphology and Protein-Production in Chemostat Cultures of Recombinant Aspergillus-Oryzae. *Biotechnology and Bioengineering*, **62**, 4, 434-446.

Amaral, A.L., Baptiste, C., Pons, M.N., Nicolau, A., Lima, N., Ferreira, E.C., Mota, M. and Vivier, H. (1999) Semiautomated Recognition of Protozoa by Image-Analysis. *Biotechnology Techniques*, **13**, 2, 111-118.

Atenas, M., Clark, M. and Lazarova, V. (1998) Characterization of bubbles in a rectangular air-lift bioreactor. *Particle and Particle Systems Characterization*, **15**, 191-199.

Barciela, J. and Vieitez, A.M. (1993) Anatomical Sequence and Morphometric Analysis During Somatic Embryogenesis on Cultured Cotyledon Explants of Camellia- Japonica L. *Annals of Botany*, **71**, 5, 395-404.

Bavarian, F., Fan, L.S. and Chalmers, J.J. (1991) Microscopic visualization of insect cell-bubble interactions. I. Rising bubbles, air-medium interface and the foam layer. *Biotechnology Progress*, **7**, 140-150.

Bellouti, M., Alves, M., Novais, J.M. and Mota, M. (1997) Flocs versus Granules: Differentation by Fractal Dimension. *Water Research*, **31**, 5, 1227-1231.

Benkrid, K. (1999) Etude globale et locale de l'hydrodynamique des écoulements gaz-liquide dans les réacteurs à lit fixe, PhD thesis, INPL, Nancy, France.

Bittner, C., Wehnert, G. and Scheper, T. (1998) In Situ Microscopy for On-line Determination of Biomass. *Biotechnology and Bioengineering*, **60**, 1, 24-35.

Bonarius, H.P.J., Nielsen, N.P.V. and Kongerslev, L. Optimal Image-Analysis Software for Rapid and Reliable of Cultured-Mammalian-Cells. In *Abstracts of Papers of the American Chemical Society*, pp. 206-BIOT. Washington: American Chemical Society.

Bouaifi, M. and Roustan, M. (1998) Bubble size and mass transfer coefficients in dual-impeller agitated reactors. *Canadian Journal of Chemical Engineering*, **76**, 390-397.

Boulton-Stone, J.M. and Blake, J.R. (1993) Bursting bubbles at a free-surface. *Proc. 3rd Int. Conf. Bioreactor and Bioprocess Fluid Dynamics*, A.W. Nienow Ed., 163-173, London: MEP Ltd.

Brodatz, P. (1966) *Textures*, New York: Dover Publications.

Bujalski, W., Takenaka, K., Paolini, S., Jahoda, M., Paglianti, A., Takahashi, K., Nienow, A.W. and Etchells, A.W. (1999) Suspension and liquid homogeneization in high solids concentration stirred chemical reactors. *Transactions of the Institution of Chemical Engineers*, Part A, **77**, 241-247.

Calderbank, P.H. (1958) The interfacial area in gas-liquid contacting with mechanical agitation. *Transactions of the Institution of Chemical Engineers*, **36**, 443-463.

Cazzulino, D., Pedersen, H. and Chin, C.-K. 1991, Bioreactors and Image Analysis for Scale-Up and Plant Propagation. In *Cell Culture and Somatic Cell*, vol. 8, pp. 147-177. San Diego: Academic Press

Chalmers, J.J. and Bavarian, F. (1991) Microscopic visualization of insect cell-bubble interactions. II: the bubble film and bubble rupture. *Biotechnology Progress*, **7**, 151-158.

Chaouki, J., Larachi, F. and Dudukovic, M.P. (1997) Noninvasive tomographic and velocimetric monitoring of multiphase flows. *Industrial and Engineering Chemistry Research,* **36**, 4476-4503.

Chi, C.M., Zhang, C., Staba, E.J., Cooke, T.J. and Hu, W.S. (1996) An Advanced Image-Analysis System for Evaluation of Somatic Embryo Development. *Biotechnology and Bioengineering*, **50**, 1, 65-72.

Choi, D.B., Park, E.Y. and Okabe, M. (1998) Improvement of Tylosin Production from Streptomyces-Fradiae Culture by Decreasing the Apparent Viscosity in an Airlift Bioreactor. *Journal of Fermentation and Bioengineering*, **86**, 4, 413-417.

Conners, R.W. (1980) A theoretical comparison of texture algorithms. *IEEE Transactions on Pattern Analysis and Machine Intelligence*, **3**, 204-222.

Costello, P.J. and Monk, P.R. (1985) Image Analysis Method for the Rapid Counting of *Saccharomyces cerevisiae* Cells. *Applied and Environmental Microbiology*, **49**, 4, 863-866.

Cowger, N.L., O'Connor, K.C., Hammond, T.G., Lacks, D.J. and Navar, G.L. (1999) Characterization of Bimodal Cell Death of Insect Cells in a Rotating-Wall Vessel and Shaker Flask. *Biotechnology and Bioengineering*, **64**, 1, 14-26.

Cox, P.W. and Thomas, C.R. (1992) Classification and Measurement of Fungal Pellets by Automated Image Analysis. *Biotechnology and Bioengineering*, **39**, 9, 945-952.

Cox, P.W. and Thomas, C.R. (1999) Assessment of the Activity of Filamentous Fungi Using *Mag fura*. *Mycological Research*, **103**, 6, 757-763.

de Swart, J.W.A., van Vliet, R.E. and Krishna, R. (1996) Size, structure and dynamics of "large" bubbles in a two-dimensional slurry bubble column. *Chemical Engineering Science*, **51**, 4619-4629.

DiBiasio, D., Scott, J., Harris, P. and Moore S. (1993) The relationship between fluid flow and cell growth in hollow-fiber bioreactors: applications of magnetic resonance imaging. *Proc. 3rd Int. Conf. Bioreactor and Bioprocess Fluid Dynamics*, A.W. Nienow Ed., 457-471, London: MEP Ltd.

Doran, P. (1999) Design of mixing systems for plant cell suspensions in stirred reactors. *Biotechnology Progress*, **15**, 319-335.

Drouin, J.F., Louvel, L., Vanhoutte, B., Vivier, H., Pons, M.N. and Germain, P. (1997) Quantitative Characterization of Cellular Differentiation of Streptomyces ambofaciens in Submerged Culture by Image Analysis. *Biotechnology Techniques*, **11**, 11, 819-824.

Dubuisson, M.P., Jain, A.K. and Jain, M.K. (1994) Segmentation and Classification of Bacterial Culture Images. *Journal of Microbiological Methods*, **19**, 4, 279-295.

Dudley, B.T., Howgrave-Graham, A.R., Bruton, A.G. and Wallis, F.M. (1993) Image Analysis to Quantify and Measure UASB Digester Granules. *Biotechnology and Bioengineering*, **42**, 3, 279-283.

Durant, G., Cox, P.W., Formisyn, P. and Thomas, C.R. (1994) Improved Image Analysis Algorithm for the Characterization of Mycelial Aggregates after Staining. *Biotechnology Techniques*, **8**, 11, 759-764.

Durant, G., Crawley, G. and Formisyn, P. (1994) A Simple Staining Procedure for the Characterisation of *Basidiomycetes* Pellets by Image Analysis. *Biotechnology Techniques*, **8**, 6, 395-400.

Einax, J.W., Zwanziger, H.W. and Geiss, S. (1997) *Chemometrics in Environmental Analysis*, Weinheim: VCH.

Galindo, E. and Nienow, A.W. (1992) Mixing of highly viscous xanthan fermentation broths with Lightnin A315 impeller. *Biotechnology Progress*, **8**, 233-239.

Galindo, E. and Nienow, A.W. (1993) Performance of the SCABA SRGT agitator in mixing of simulated xanthan gum broths. *Chemical Engineering and Technology*, **16**, 102-108.

Garcia-Briones, M.A. and Chalmers, J.J. (1993) Analysis of hydrodynamic information obtained from computer solutions of the rupture of a gas bubble in relation to animal cell damage in sparged biroeactors. *Proc. 3rd Int. Conf. Bioreactor and Bioprocess Fluid Dynamics*, A.W. Nienow Ed., 191-210, London: MEP Ltd.

Gobal, M. and Jepson, W. (1997) Development of digital image analysis techniques for the study of velocity and void profiles in slug flow. *International Journal of Multiphase Flow*, **23**, 945-965.

Godfroy, L., Larachi, F., Kennedy, G., Grandjean, B.P.A. and Chaouki, J. (1997) On-line flow visualization in multiphase reactors using neural networks. *Applied Radiation and Isotopes*, **48**, 225-235.

Grijspeerdt, K. and Verstraete, W. (1997) Image Analysis to Estimate the Settleability and Concentration of Activated Sludge. *Water Research*, **31**, 5, 1126-1134.

Guterman, H. and Shabtai, Y. (1996) A Self-Tuning Vision System for Monitoring Biotechnological Processes. I. Application to Production of Pullulan by Aureobasidium pullulans. *Biotechnology and Bioengineering*, **51**, 501-510.

Haralick, R.M. (1979) Statistical and structural approaches to texture. *Proceedings of the IEEE*, **67**, 786-804.

Hari-Prajitno D., Mishra V.P., Takenaka, K., Bujalski, W., Nienow, A.W. and McKemme, J. (1998) Gas-liquid mixing studies with multiple up- and down-pumping hydrofoil impellers: power characteristics and mixing time. *Canadian Journal of Chemical Engineering*, **76**, 1056-1068.

Harrell, R.C., Bieniek, M. and Cantliffe, D.J. (1992) Noninvasive Evaluation of Somatic Embryogenesis. *Biotechnology and Bioengineering*, **39**, 4, 378-383.

Higashiyama, K., Fujikawa, S., Park, E.Y. and Okabe, M. (1999) Image Analysis of Morphological Change During Arachidonic Acid Production by *Mortierella alpina* 1S-4. *Journal of Bioscience and Bioengineering*, **87**, 4, 489-494.

Hirano, T. (1990) Method for Measuring the Budding Index of Yeast Using an Image Processor. *ASBC Journal*, **48**, 2, 79-81.

Holden, P.J., Wang, M., Mann, R., Pickin, F.J. and Edwards, R.B. (1998) Imaging stirred-vessel macromixing using electrical resistance tomography. *AIChE Journal*, **44**, 780-790.

Honda, H., Ito, T., Yamada, J., Hanai, T., Matsuoka, M. and Kobayashi, T. (1999) Selection of Embryogenic Sugarcane Callus by Image Analysis. *Journal of Bioscience and Bioengineering*, **87**, 5, 700-702.

Houcine, I., Vivier, H., Plasari, E., David, R. and Villermaux, J. (1996) Planar laser induced fluorescence technique for measurements of concentration fields in continuous stirred tank reactors. *Experiments in Fluids*, **22**, 95-102.

Hsieh, C.C., Wang, S.B. and Pan, C. (1997) Dynamic visualization of two-phase flow patterns in a natural ciculation loop. *International Journal of Multiphase Flow*, **6**, 1147-1170.

Jenkins, D., Richard, M.G. and Daigger, G.T. (1993) *Manual on the Causes and Control of Activated Sludge Bulking and Foaming*, 2nd edn. Chelsea: Lewis Publishers.

Jüsten, P., Paul, G.C., Nienow, A.W. and Thomas, C.R. (1996) Dependence of Mycelial Morhology on Impeller Type and Agitation Intensity. *Biotechnology and Bioengineering*, **52**, 6, 672-684.

Kamilakis, E.G. and Allen, D.G. (1995) Cultivating Filamentous Microorganisms in a Cyclone Bioreactor - The Influence of Pumping on Cell Morphology. *Process Biochemistry*

Kandel, E.R., Schwartz, J.H. and Jessel, T.M. (1995) *Essentials of Neural Science and Behaviour*, New Jersey: Prentice-Hall.

Kaneshiro, E.S., Wyder, M.A., Wu, Y.P. and Cushion, M.T. (1993) Reliability of Calcein Acetoxy Methyl-Ester and Ethidium Homodimer or Propidium Iodide for Viability Assessment of Microbes. *Journal of Microbiological Methods*, **17**, 1, 1-16.

Kawaharasaki, M., Tanaka, H., Kanagawa, T. and Nakamura, K. (1998) In Situ Identification of Polyphosphate-Accumulating bacteria in Activated Sludge by Dual Staining with rRNA-targeted Olignucleotide Probes and 4',6'-Diamidino-2-Phenylindol (DAPI) at a Polyphosphate-Probing Concentration. *Water Research*, **33**, 1, 527-265.

Kieran, P.M., Malone, D.M. and Macloughlin, P.F. (1993) Variation of Aggregate Size in Plant-Cell Suspension Batch and Semicontinuous Cultures. *Food and Bioproducts Processing*, **71**, C1, 40-46.

Kieran, P.M., Odonnell, H.J., Malone, D.M. and Macloughlin, P.F. (1995) Fluid Shear Effects on Suspension-Cultures of Morinda-Citrifolia. *Biotechnology and Bioengineering*, **45**, 5, 415-425.

Konstantinov, K., Chuppa, S., Sajan, E., Tsai, Y., Yoon, S. and Golini, F. (1994) Real-time Biomass-concentration monitoring in Animal-cell Cultures. *Trends in Biotechnology*, **12**, 324-333.

Kuehn, M., Hausner, M., Bungartz, H.J., Wagner, M., Wilderer, P.A. and Wuertz, S. (1998) Automated Confocal Laser Scanning Microscopy and Semiautomated Image Processing for Analysis of Biofilms. *Applied and Environmental Microbiology*, **64**, 11, 4115-4127.

Kumar, S.B. and Dudukovic, M.P. (1997) Computer-assisted gamma and X-ray tomography: application to multiphase flow. In *Non-invasive Monitoring of Multiphase Flows*. Chaouki, J., Larachi, F., Dudukovic, M.P., Eds., Amsterdam: Elsevier.

Lawrence, J.R., Nie, T.R. and Swerhone, G.D.W. (1998) Application of Multiple Parameter Imaging for the Quantification of Algal, Bacterial and Exopolymer Components of Microbial Biofilms. *Journal of Microbiological Methods*, **32**, 3, 253-261.

Lee, J.C., Salih, M.A., Sebai, N.N. and Withey, A. (1993) Control of foam in bioreactors – action of antifoams. *Proc. 3rd Int. Conf. Bioreactor and Bioprocess Fluid Dynamics*, A.W. Nienow Ed., 275-287, London: MEP Ltd.

Lee, N., Nielsen, P.H., Andreasen, K.H., Juretschko, S., Nielsen, J.L., Schleifer, K.H. and Wagner, M. (1999) Combination of Fluorescent in-Situ Hybridization and Microautoradiography - A New Tool for Structure-Function Analyses in Microbial Ecology. *Applied and Environmental Microbiology*, **65**, 3, 1289-1297.

Leondes, C.T. (1993) *Image Processing and Pattern Recognition*, San Diego: Academic Press.

Li, H.Z., Mouline, Y., Choplin, L. and Midoux, N. (1997) Chaotic bubble coalescence in no-newtonian fluids. *International Journal of Multiphase Flow*, **23**, 713-723.

Li, L. and Wei, J. (1999) Three-dimensional image analysis of mixing in stirred vessels. *AIChE Journal*, **45**, 1855-1865.

Logothetis, N.K. (1999) Vision: A Window on Consciousness, *Scientific American*, 281, 5, 45-51.

Lumley, D.J. and Horkeby, G. (1989) Retention time distribution of sludge in rectangular secondary settlers. *Water Science and Technology*, **21**, 1763-1766.

Madoni, P. (1994) A Sludge Biotic Index (Sbi) for the Evaluation of the Biological Performance of Activated-Sludge Plants Based on the Microfauna Analysis. *Water Research*, **28**, 1, 67-75.

Makagiansar, H.Y., Ayazi Shamlou, P., Thomas, C.R. and Lilly, M.D. (1993) The Influence of Mechanical Forces on the Morphology and Penicillin Production of *Penicillium chrysogenum*. *Bioprocess Engineering*, **9**, 83-90.

Margaritis, A., te Bokkel D.W. and Karamanev, D.G. (1999) Bubble rise velocities and drag coefficients in non-newtonian polysaccharide solutions. *Biotechnology and Bioengineering*, **64**, 257-266.

Maruhashi, F., Murakami, S. and Baba, K. (1994) Automated Monitoring of Cell Concentration and Viability Using an Image-Analysis System. *Cytotechnology*, **15**, 1-3, 281-289.

Mccarthy, A.A., O'Shea, D.G., Murray, N.T., Walsh, P.K. and Foley, G. (1998) Effect of Cell Morphology on Dead-End Filtration of the Dimorphic Yeast Kluyveromyces-Marxianus Var. Marxianus NRRLy2415. *Biotechnology Progress*, **14**, 2, 279-285.

Mcintyre, M. and Mcneil, B. (1997a) Dissolved Carbon-Dioxide Effects on Morphology, Growth, and Citrate Production in Aspergillus-Niger A60. *Enzyme and Microbiology Technology*, **20**, 2, 135-142.

Mcintyre, M. and Mcneil, B. (1997b) Effect of Carbon-Dioxide on Morphology and Product Synthesis in Chemostat Cultures of Aspergillus-Niger A60. *Enzyme and Microbiology Technology*, **21**, 7, 479-483.

Moolman, D.W., Aldrich, C., Van Deventer, J.S.J. and Stange, W.W. (1994) Digital image processing as a tool for on-line monitoring of froth in flotation froths. *Minerals Engineering*, 7, 9, 1149-1164.

Moravec, H. (1999) Rise of Robots. *Scientific American*, 281, 6, 86-93.

Mouline, Y. (1996) Dynamique des bulles de gaz dans les fluides rhéologiquement complexes, PhD thesis, INPL, Nancy, France.

Nielsen, J. and Krabben, P. (1995) Hyphal Growth and Fragmentation of Penicillium-Chrysogenum in Submerged Cultures. *Biotechnology and Bioengineering*, **46**, 6, 588-598.

Nielsen, J. (1996) Modeling the Morphology of Filamentous Microorganisms. *Trends in Biotechnology*, **14**, 11, 438-443.

Nielsen, J., Johansen, C.L., Jacobsen, M., Krabben, P. and Villadsen, J. (1995) Pellet Formation and Fragmentation in Submerged Cultures of Penicillium-Chrysogenum and Its Relation to Penicillin Production. *Biotechnology Progress*, **11**, 1, 93-98.

Nielsen, P.H., Andreasen, K., Lee, N. and Wagner, M. (1999) Use of Microautoradiography and Fluorescent in situ Hybridization for Characterization of Microbial Activity in Activated Sludge. *Water Science and Technology*, **39**, 1, 1-9.

Olsvik, E., Tucker, K.G., Thomas, C.R. and Kristiansen, B. (1993) Correlation of *Aspergillus niger* Broth Rheological Properties with Biomass Concentration and the Shape of Mycelial Aggregates. *Biotechnology and Bioengineering*, **42**, 9, 1046-1052.

O'Shea, D.G. and Walsh, P.K. (1996) Morphological Characterization of the Dimorphic Yeast Kluyveromyces-Marxianus Var Marxianus Nrrly2415 by Semiautomated Image-Analysis. *Biotechnology and Bioengineering*, **51**, 6, 679-690.

Pandit, A.B., Dodd, P.W. and Davidson, J.F. (1993) The effect of immersed tubes on bubble size in an air-lift fermenter. *Proc. 3rd Int. Conf. Bioreactor and Bioprocess Fluid Dynamics*, A.W. Nienow Ed., 213-232, London: MEP Ltd.

Paul, G.C., Kent, C.A. and Thomas, C.R. (1994) Image-Analysis for Characterizing Differentiation of *Penicillium chrysogenum*. *Transactions of the Institution of Chemical Engineers, Part C*, **72**, 2, 95-105.

Perrier-Cornet, J.-M., Maréchal, P.-A. and Gervais, P. (1995) A New Design Intended to Relate High Pressure Treatment to Yeast Cell Mass Transfer. *Journal of Biotechnology*, **41**, 49-58.

Pichon, D., Vivier, H. and Pons, M.N. (1992) Growth Monitoring of Mammalian Cells on Microcarriers by Image Analysis. In *Modeling and Control of Biotechnical Processes*, edited by M. Nazmul Karim, G. Stephanopoulos, pp. 311-314. Oxford: Pergamon Press.

Pichon, D., Vivier, H. and Pons, M.N. (1992) Growth Monitoring of Filamentous Microorganisms by Image Analysis. In *Modeling and Control of Biotechnical Processes*, edited by M. Nazmul Karim, G. Stephanopoulos, pp. 307-310. Oxford: Pergamon Press.

Pitiot, P., Falk, L. and Vivier, H. (1998) Caractérisation, par trajectographie tridimensionnelle, du mélange dans un réacteur agité ouvert. *Récents Progrès en génie des Procédés*, **12**, 61, 103-108.

Pons, M.N., Drouin, J.F., Louvel, L., Vanhoutte, B., Vivier, H. and Germain, P. (1998) Physiological Investigations by Image-Analysis. *Journal of Biotechnology*, **65**, 1, 3-14.

Pons, M.N., Vivier, H., Rémy, J.F. and Dodds, J.A. (1993) Morphological Characterization of Yeast by Image Analysis. *Biotechnology and Bioengineering*, **42**, 1352-1359.

Pons, M.N., Wagner, A., Vivier, H. and Marc, A. (1992) Application of Quantitative Image Analysis to a Mammalian Cell Line Grown on Microcarriers. *Biotechnology and Bioengineering*, **40**, 1, 187-193.

Pons, M.N., Vivier, H., Belaroui, K., Bernard-Michel, B., Cordier, F., Oulhana, D. and Dodds, J.A. (1999) Particle morphology: from visualisation to measurement. *Powder Technology*, **103**, 44-57.

Priede, M.A., Vanags, J.J., Viesturs, U.E., Tucker, K.G., Bujalski, W. and Thomas, C.R. (1995) Hydrodynamic, Physiological, and Morphological Characteristics of *Fusarium moniliforme* in Geometrically Dissimilar Stirred Bioreactors. *Biotechnology and Bioengineering*, **48**, 3, 266-277.

Rayleigh, J.W. (1891) Some applications of photography, *Nature*, **44**, 249-254.

Reichl, U., King, R. and Gilles, E.D. (1992) Characterization of Pellet Morphology During Submerged Growth of *Streptomyces tendae* by Image Analysis. *Biotechnology and Bioengineering*, **39**, 2, 164-170.

Reinecke, N., Petritsch, G., Boddem, M. and Mewes, D. (1998) Tomographic imaging of the phase distribution in two-phase slug flow. *International Journal of Multiphase Flow*, **24**, 617-634.

Ren, J., Reid, J.F. and Litchfield, J.B. (1994) Knowledge-based Supervision and Control of Bioprocess with a Machine Vision-based Sensing System. *Journal of Biotechnology*, **36**, 1, 25-34.

Ruaan, R.C., Tsai, G.J. and Tsao, G.T. (1993) Monitoring and Modeling Density-Dependent Growth of Anchorage- Dependent Cells. *Biotechnology and Bioengineering*, **41**, 3, 380-389.

Ryoo, D. (1999) Fungal Fractal Morphology of Pellet Formation in *Aspergillus niger*. *Biotechnology Techniques*, **13**, 1, 33-36.

Sardonini, C.A. and DiBiaso, D. (1993) Growth of animal cells around hollow fibers – Multifiber studies. *AIChE Journal*, **39**, 1415-1419.

Sarker, D.K., Bertrand, D., Chtioui, Y. and Popineau, Y. (1998) Characterisation of foam properties using image analysis. *Journal of Texture Studies*, **29**, 15-42.

Schaflinger, U., Acrivos, A. and Zhang, K. (1990) Viscous resuspension of a sediment within a laminar and stratified flow. *International Journal of Multiphase Flow*, **16**, 567-578.

Schmidt, J. and Lübbert, A. (1993). Detailed investigation of the mass transfer between bubbles and the continuous liquid phase. *Proc. 3rd Int. Conf. Bioreactor and Bioprocess Fluid Dynamics*, A.W. Nienow Ed., 231-239, London: MEP Ltd.

Sebastine, I.M., Stocks, S.M., Cox, P.W. and Thomas, C.R. (1999) Characterisation of Percentage Viability of *Streptomyces clavuligerus* Using Image Analysis. *Biotechnology Techniques*, **13**, 419-423.

Sekiguchi, Y., Kamagata, Y., Nakamura, K., Ohashi, A. and Harada, H. (1999) Fluorescence in-Situ Hybridization Using 16S Ribosomal-RNA- Targeted Oligonucleotides Reveals Localization of Methanogens and Selected Uncultured Bacteria in Mesophilic and Thermophilic Sludge Granules. *Applied and Environmental Microbiology*, **65**, 3, 1280-1288.

Semmens, M.J., Gulliver, J.S. and Anderson, A. (1999) An analysis of bubble formation using microporous hollow fiber membranes. *Water Environment Research*, **71**, 307-315.

Singh, A., Pyle, B.H. and McFeters, G.A. (1989) Rapid Enumeration of Viable Bacteria by Image Analysis. *Journal of Microbiological Methods*, **10**, 91-101.

Smith, M.A.L., Reid, J.F., Hansen, A.C. and Madhavi, D.L. (1995) Non-destructive Machine Vision Analysis of Pigment-Producing Cell Cultures. *Journal of Biotechnology*, **40**, 1-11.

Suhr, H., Wehnert, G., Schneider, K., Geissler, P., Jahne, B. and Scheper, T. (1995) In Situ Microscopy for On-line Characterization of Cell-Populations in Bioreactors, Including Cell-Concentration Measurments by Depth from Focus. *Biotechnology and Bioengineering*, **47**, 106-116.

Swope, K.L. and Flicklinger, M.C. (1996) The Use of Confocal Scanning Laser Microscopy and Other Tools to Characterize Escherichia-Coli in a High-Cell-Density Synthetic Biofilm. *Biotechnology and Bioengineering*, **52**, 2, 340-356.

Takahashi, K. and Nienow, A.W. (1988) Bubble sizes, gas hold-up and coalescence rates in aerated vessels agitated by a Rushton turbine: spatial variations. *Proc. 6th European Conf. On Mixing*, 285-293, Pavia, Italy.

Tamura, S., Park, Y., Toriyama, M. and Okabe, M. (1997) Change of Mycelial Morphology in Tylosin Production by Batch Culture of Streptomyces-Fradiae Under Various Shear Conditions. *Journal of Fermentation and Bioengineering*, **83**, 6, 523-528.

Tan, W.S., Chen, Y.L. and Dai, G.C. (1993) Growth and damage of continuous suspension cultured hybrydoma cells (2F7) in an agitated bioreactor with and without bubble entrainment or sparging. *Proc. 3rd Int. Conf. Bioreactor and Bioprocess Fluid Dynamics*, A.W. Nienow Ed., 153-161, London: MEP Ltd.

Tatterson, G.B. (1991) Fluid mixing and gas dispersion in agitated tanks, NewYork: McGraw Hill.

Thomas, C.R. (1992) Image-Analysis - Putting Filamentous Microorganisms in the Picture. *Trends in Biotechnology*, **10**, 10, 343-348.

Treskatis, S.-K., Orgeldinger, V., Wolf, H. and Gilles, E.D. (1997) Morphological Characterization of Filamentous Microorganisms in Submerged Cultures by On-Line Digital Image Analysis and Pattern Recognition. *Biotechnology and Bioengineering*, **53**, 2, 191-201.

Tucker, K.G. and Thomas, C.R. (1993) Effect of Biomass Concentration and Morphology on the Rheological Parameters of *Penicillium chrysogenum* Fermentation Broths. *Transactions of the Institution of Chemical Engineers, Part C*, **71**, June, 111-117.

Tucker, K.G., Chalder, S., Alrubeai, M. and Thomas, C.R. (1994) Measurement of Hybridoma Cell Number, Viability, and Morphology Using Fully Automated Image-Analysis. *Enzyme and Microbial Technology*, **16**, 1, 29-35.

Tucker, K.G., Kelly, T., Delgrazia, P. and Thomas, C.R. (1992) Fully-Automatic Measurement of Mycelial Morphology by Image Analysis. *Biotechnology Progress*, **8**, 4, 353-359.

Uozumi, N., Yoshino, T., Shiotani, S., Suehara, K.I., Arai, F., Fukuda, T. and Kobayashi, T. (1993) Application of Image Analysis with Neural Network for Plant Somatic Embryo Culture. *Journal of Fermentation and Bioengineering*, **76**, 6, 505-509.

Vanhoutte, B., Pons, M.N., Thomas, C.R., Louvel, L. and Vivier, H. (1995) Characterization of Penicillium chrysogenum Physiology in Submerged Cultures by Color and Monochrome Image Analysis. *Biotechnology and Bioengineering*, **48**, 1-11.

Venkat, R.V., Brodkey R.S., Guezennec, Y.G. and Chalmers, J.J. (1993) Experimental determination of local hydrodynamic information in microcarrier culture spinner vessels. *Proc. 3rd Int. Conf. Bioreactor and Bioprocess Fluid Dynamics*, A.W. Nienow Ed., 483-501, London: MEP Ltd.

Vicente, A., Meinders, J.M. and Teixeira, J.A. (1996) Sizing and Counting of *Saccharomyces cerevisiae* Floc Populations by Image Analysis, Using an Automatically Calculated Threshold. *Biotechnology and Bioengineering*, **51**, 6, 673-678.

Walsby, A.E. and Avery, A. (1996) Measurement of Filamentous Cyanobacteria by Image Analysis. *Journal of Microbiological Methods*, **26**, 11-20.

Walsh, P.K., Isdell, F.V., Noone, S.M., Odonovan, M.G. and Malone, D.M. (1996) Growth-Patterns of Saccharomyces-Cerevisiae Microcolonies in Alginate and Carrageenan Gel Particles - Effect of Physical and Chemical-Properties of Gels. *Enzyme and Microbial Technology*, **18**, 5, 366-372.

Wierzba, A., Reichl, U., Turner, R.F.B., Warren, R.A.J. and Kilburn, D.G. (1995) Adhesion of Mammalian Cells to a Recombinant Attachment Factor, CBD/RGD, Analyzed by Image Analysis. *Biotechnology and Bioengineering*, **46**, 185-193.

Wittmer, S., Vivier, H., Falk, L. and Villermaux, J. (1995) Three-dimensional long-term particle tracking in a stirred tank. *Proc. 7th Int. Symposium on Flow Visualisation*, 623-633.

Yamashita, Y., Kuwashima, M., Nonaka, T. and Suzuki, M. (1993) On-line Measurement of Cell Size Distribution and Concentration of Yeast by Image Processing. *Journal of Chemical Engineering of Japan*, **26**, 6, 615-619.

Yang, Y.K., Morikawa, M., Shimizu, H., Shioya, S., Suga, K.I., Nihira, T. and Yamada, Y. (1996) Image Analysis of Mycelial Morphology in Virginiamycin Production by Batch Culture of *Streptomyces virginiae*. *Journal of Fermentation and Bioengineering*, **81**, 1, 7-12.

Zalewski, K. and Buchholz, R. (1996) Morphological Analysis of Yeast Cells Using an Automated Image Processing System. *Journal of Biotechnology*, **48**, 43-49.

Table 1. Applications to fungi

Microorganism	Comments	Reference
Penicillium chrysogenum	Morphology characterisation	Tucker et al (1992)
	Rheology	Makagiansar et al (1993)
		Tucker and Thomas (1993)
	Morphology kinetics in repeated fed-batch	Nielsen et al (1995)
		Nielsen & Krabben (1995)
	Mixing; rheology	Jüsten et al (1996)
Penicillium roqueforti	Morphology classification	Pichon, Vivier & Pons (1992)
Aspergillus niger	Pellets	Cox & Thomas (1992)
	Rheology	Olsvik et al (1993)
	Cyclone bioreactor	Kamilakis & Allen (1995)
	Carbon dioxide effect	Mcintyre & Mcneil (1997a)
		Mcintyre & Mcneil (1997b)
	Fractal dimension of pellets	Ryoo (1999)
Aspergillus oryzae	Rheology	Amanullah et al (1999)
Mortierella alpina	Morphology classification; pilot-scale	Higashiyama et al (1999)
Fusarium moniliforme	Mixing	Priede et al (1995)

Table 2. Applications to filamentous bacteria

Microorganism	Comments	Reference
Streptomyces tendae	Morphology classification	Reichl, King & Gilles (1992)
		Treskatis et al (1997)
Streptomyces virginiae	Morphology classification	Yang et al (1996)
Streptomyces ambofaciens	Filament characterisation	Pons et al (1998)
Streptomyces fradiae	Rheology	Tamura et al (1997)
		Choi, Park & Okabe (1998)
Oscillatoria rubescens	Filament characterisation	Walsby and Avery (1996)
Anabaena flos-aquae		

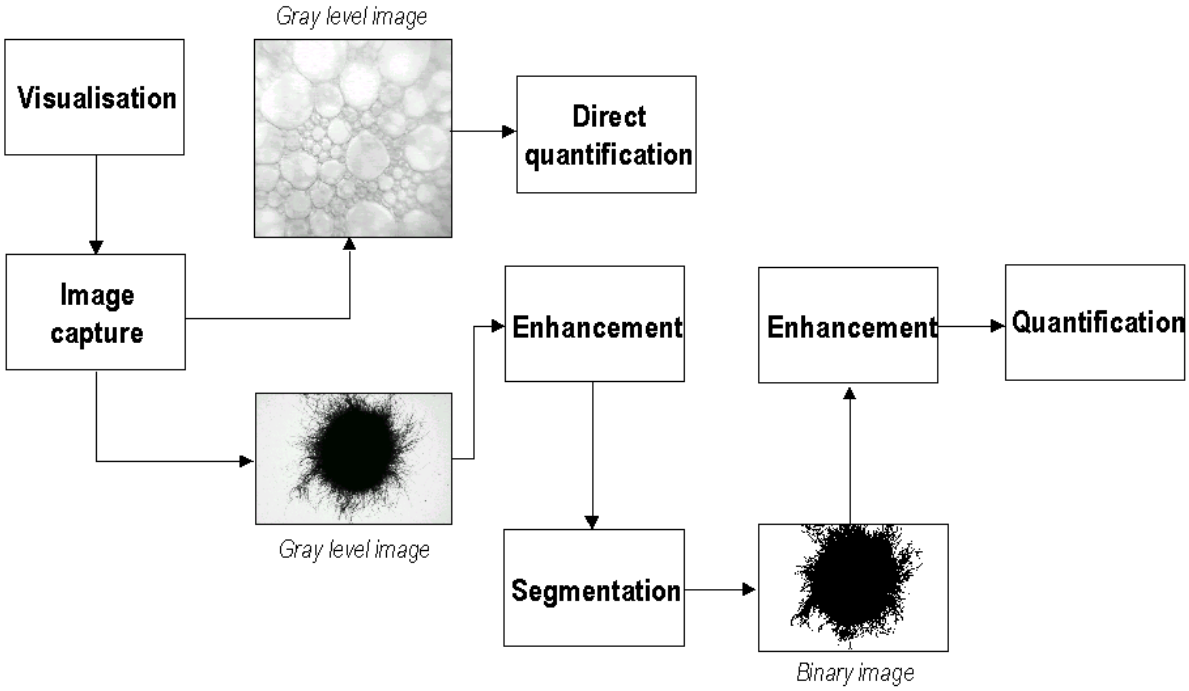

Figure 1: Principle of image processing.

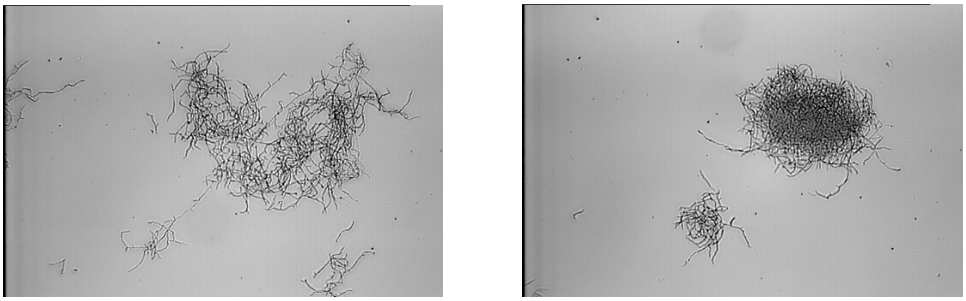

(a) (b)

Figure 2: Streptomyces ambofaciens: a) dispersed mycelia; b) pellet.

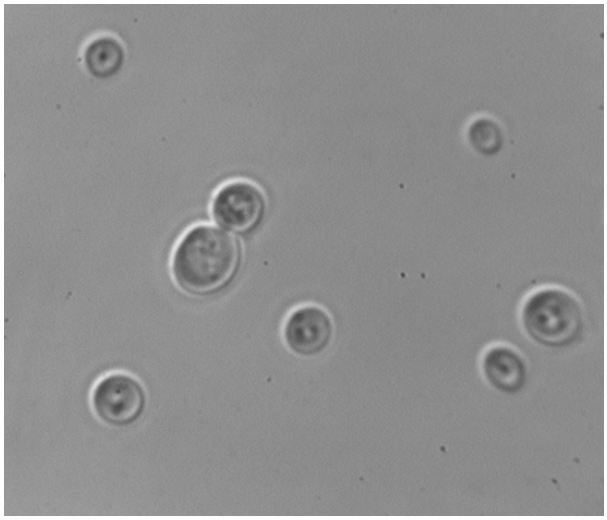

Figure 3: Saccharomyces cerevisiae yeast cell.

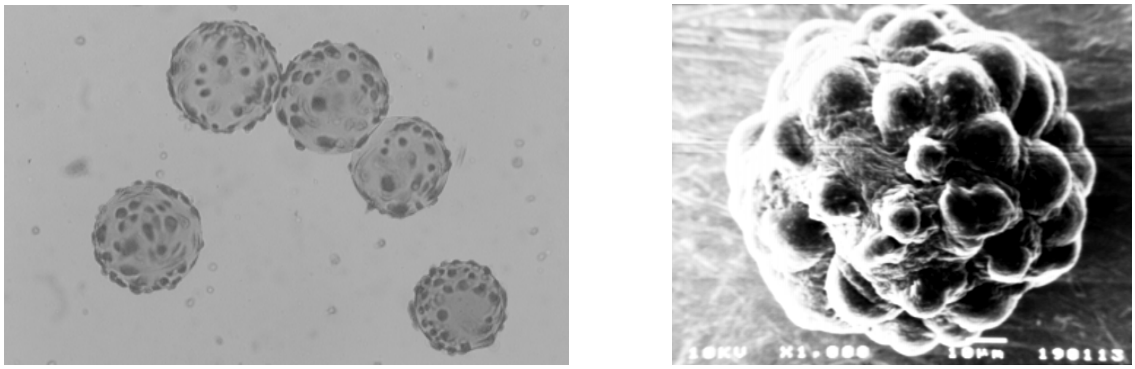

(a) (b)

Figure 4: Mammalian cells on microcarrier: a) optical microscopy; b) scanning electron microscopy.

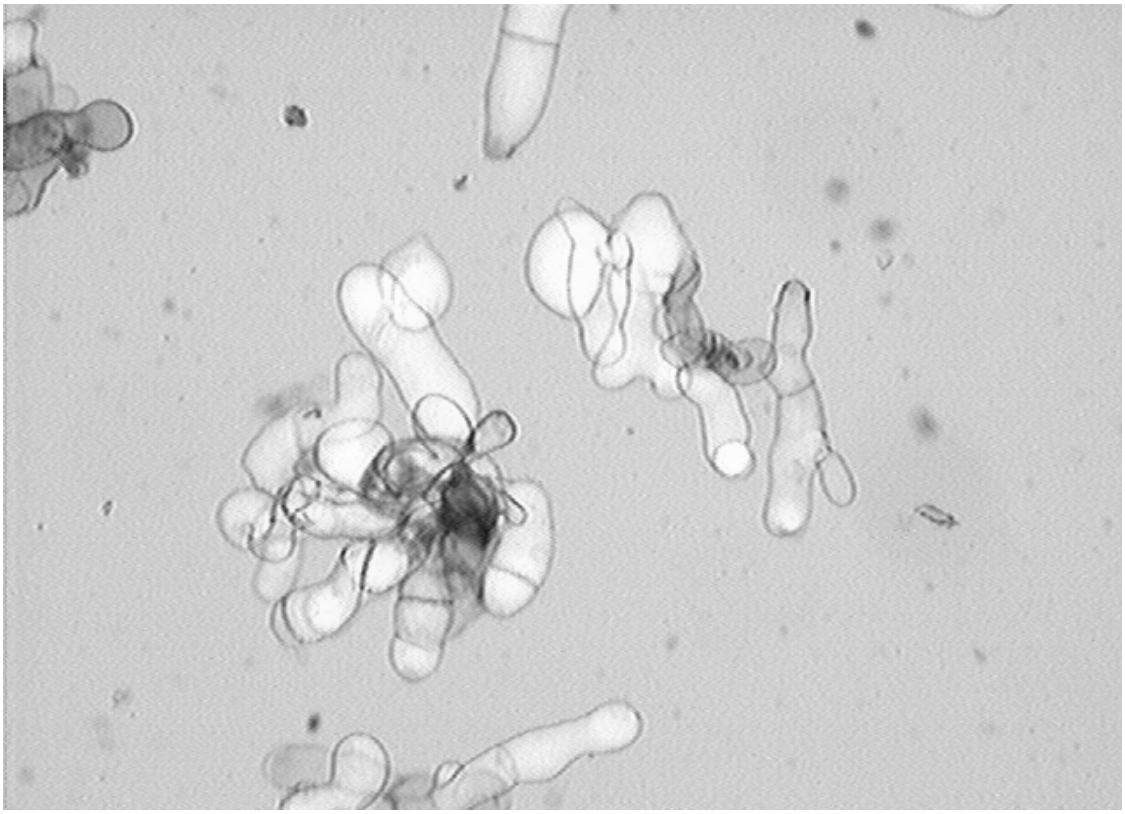

Figure 5: Suspension of somatic embryos of Pinnus pinaster (courtesy of A. Dias).

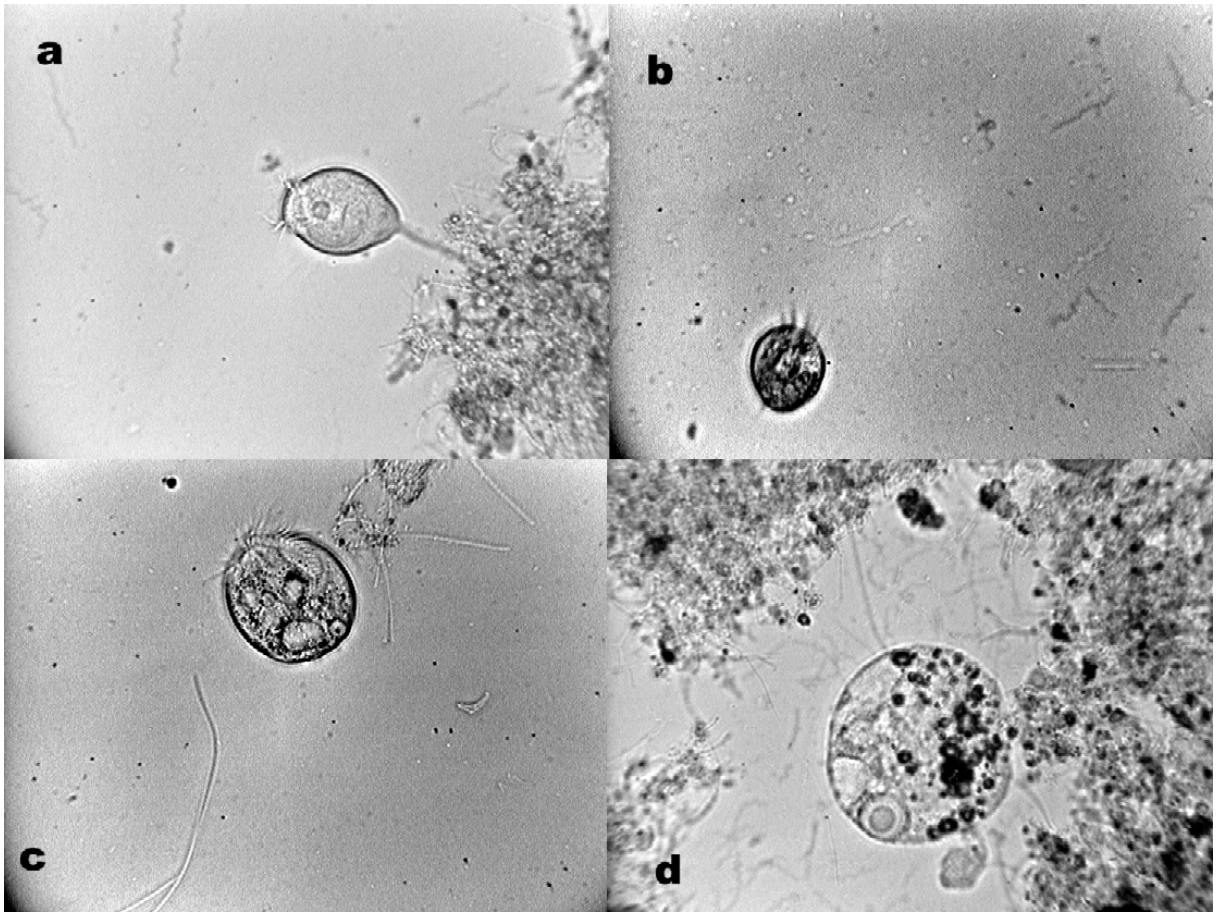

Figure 6: Protozoa in activated sludge from a wastewater treatment reactor: a) *Vorticella microstoma*, b) *Euplotes*, c) *Glaucoma*, d) *Prorodon*.

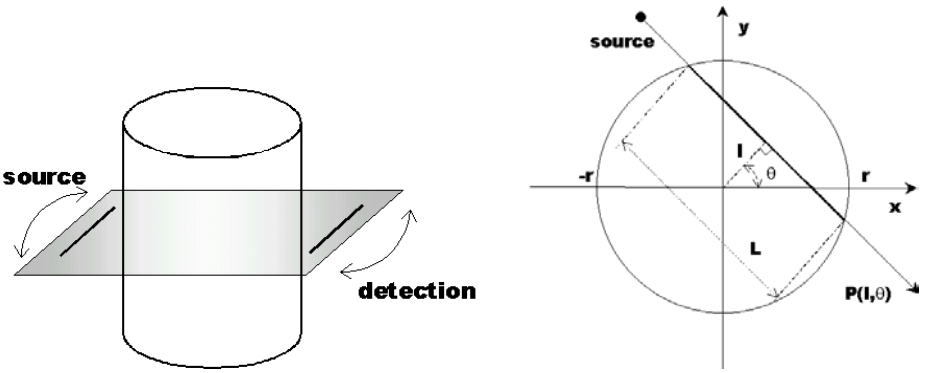

(a) (b)

Figure 7:(a) Principle of tomography and radiography; (b) 3D reconstruction from a 2D projection

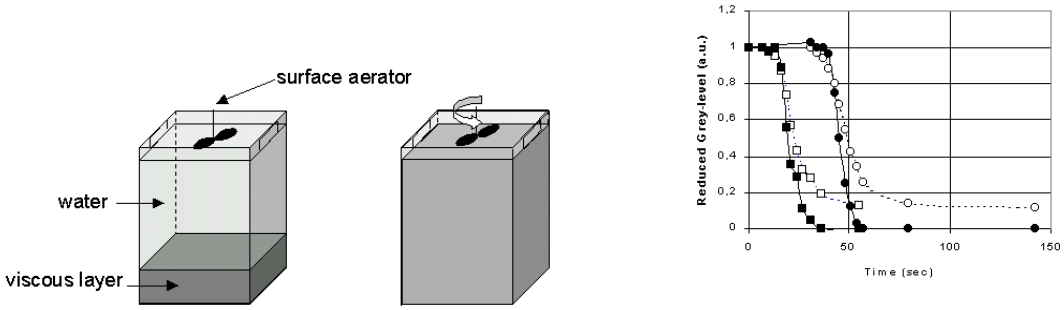

(a) (b)

Figure 8: (a) Experimental set-up of the simulated sludge resuspension test; (b) Comparison of the resuspension kinetics with a Rushton turbine. CMC concentration: 10 g/l (■, ❑) and 40 g/l (●,❍). Closed symbols for the area of interest (AOI) and open symbols for total field of view.

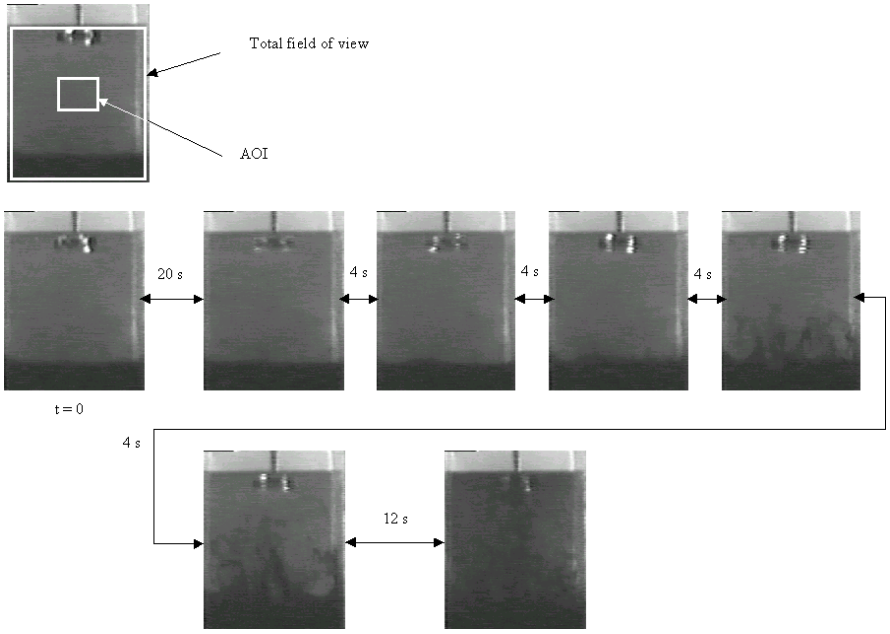

Figure 9: Some frames of the experiment with a Rushton turbine and a CMC concentration in the viscous layer of 40 g/l

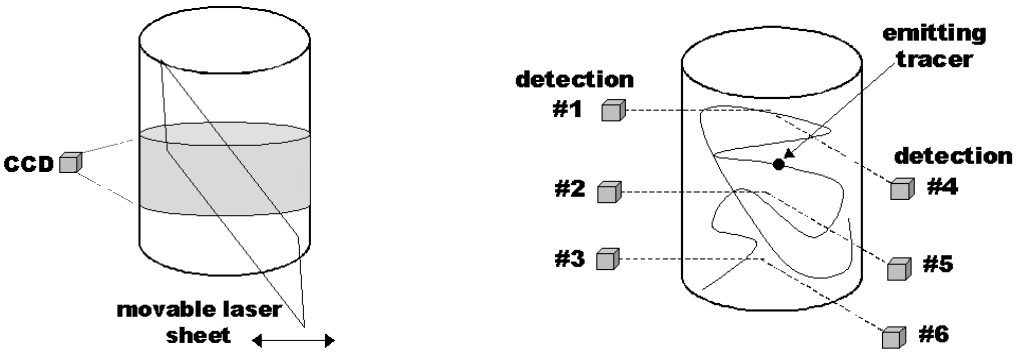

(a) (b)

Figure 10: (a) Visualisation by laser sheet illumination; (b) Radioactive particle tracking

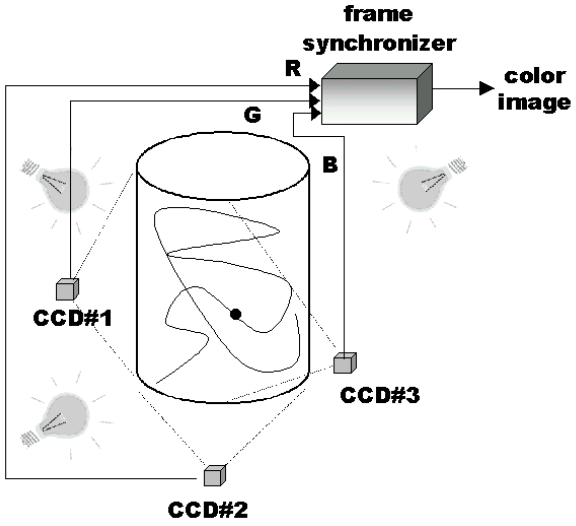

Figure 11: 3D-PTV principle

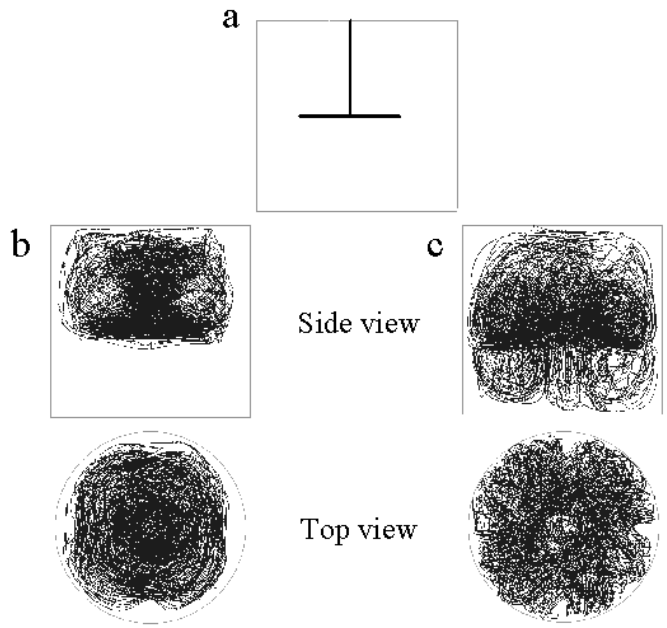

Figure 12: 3D-trajectory of the particle with a Mixel mobile and a rotation speed of 110 rpm: (a) Schematic set up; Agitation Reynolds number: 5 (b) and 56 (c); Viscosity: 5.4 Pa.s (b) and 0.14 Pa.s (c)

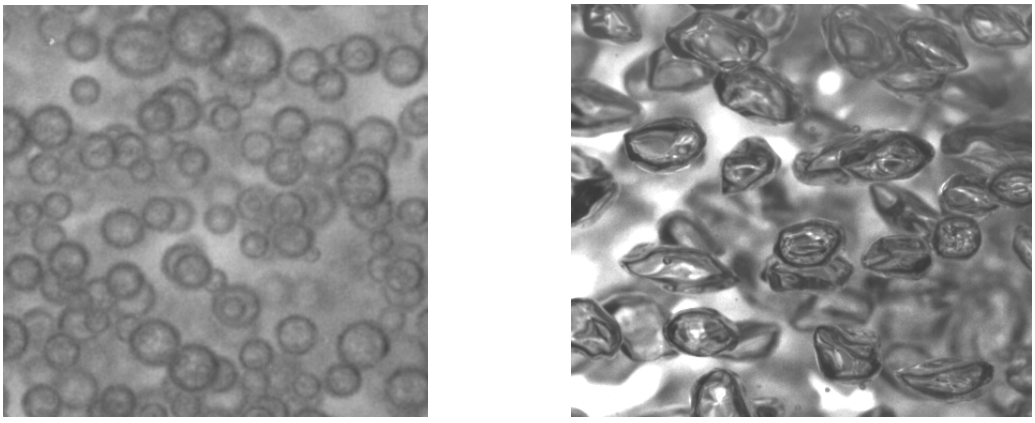

(a) (b)

Figure 13: Different shapes of bubbles in a bubble column: (a) with traces of a long-chain alcohol, (b) in pure water (*By courtesy of E. Camarasa and C. Vial*)

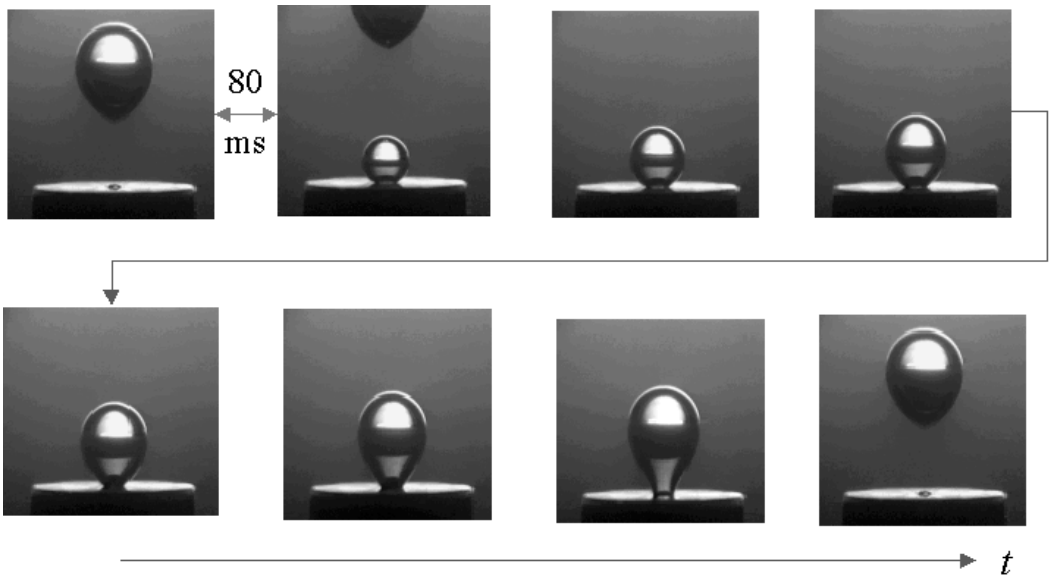

Figure 14: Generation of bubble in a viscous fluid (*by permission from Dr H.Z. Li*)

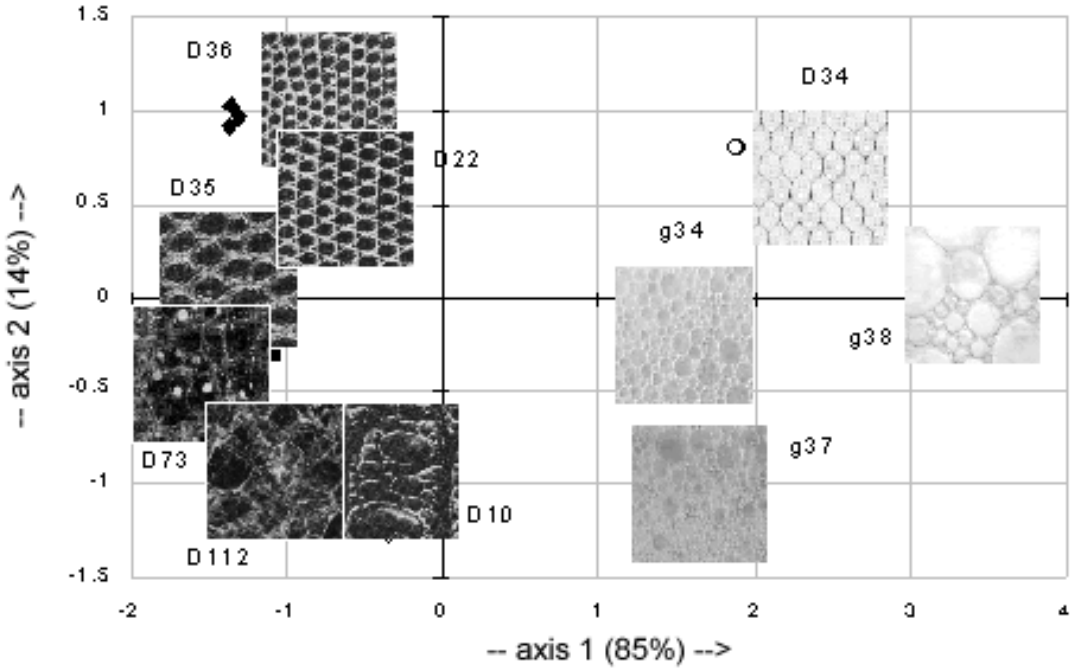

Figure 15: (●) Reference textures [Dxx from Brodatz (1966), gxx = experimental foams] for training; Validation: (▲) D3, (◊) D10, (+) D22, (❍) D34, (✶) D35, (×) D36, (❒) D73, (◆) D100, (Δ) D112